Dispersion and Rheological Aspects of SWNTs in Ultrahigh Molecular Weight Polyethylene

Qinghua Zhang,[†,§] Dirk R. Lippits,[†,‡] and Sanjay Rastogi*[,†]

Department of Chemical Engineering and Chemistry, Eindhoven University of Technology, P.O. Box 513, 5600 MB Eindhoven, The Netherlands; DSM Research, P.O. Box 18, 6160 MD, Geleen, The Netherlands; and State Key Laboratory of Chemical Fibers and Polymer Materials, College of Materials Science and Engineering, Donghua University, Shanghai 200051, P. R. China

Received May 19, 2005; Revised Manuscript Received October 27, 2005

ABSTRACT: A new method is developed to homogeneously disperse single-walled carbon nanotubes bundles (SWNTs) in an intractable polymer, for example, ultrahigh molecular weight polyethylene ($M_w > 3 \times 10^6$ g/mol) (UHMWPE). The dispersion is obtained by spraying an aqueous solution of SWNTs onto a fine UHMWPE powder directly obtained from synthesis. The SWNTs are adsorbed on the surface of the polymer powder. A composite film is prepared from the solution of the polymer powder dissolved in xylene. The high viscosity of UHMWPE in solution prevents coagulation of the adsorbed SWNTs. Scanning electron microscopy (SEM) of the films reveals that SWNT bundles are randomly dispersed in the UHMWPE matrix. The observed "shish-kebab" morphology in the SEM pictures of the film shows that the polymer chains tend to crystallize from solution as chain-folded crystals (kebab). The nanotube surface can act as a nucleating site (shish). The orientation of the dispersed SWNTs in UHMWPE matrix is achieved on solid-state drawing the solution crystallized films. Crystallization of the UHMWPE melt followed by rheometry shows that the presence of SWNTs enhances the overall crystallization rate. The observed rheological behavior of the UHMWPE/SWNT nanocomposites is rather unusual. Varying the content of SWNTs, the dynamic viscosity/storage modulus shows a minimum. The decrease in viscosity is attributed to the selective adsorption of the high molar mass fraction onto the nanotubes surface. The increase in viscosity upon further increasing the nanotube content is attributed to the formation of an elastic nanotube−polymer network. The formed nanotube−polymer network is conductive at percolation threshold of 0.6 wt % SWNTs.

1. Introduction

The discovery of carbon nanotubes (CNTs) possessing unique electronic, thermal, optical, and mechanical properties and their potential use in the next generation of composite materials has led to considerable attention in academia and industry. CNTs have the ability to affect the material properties at low loading due to their extremely high aspect ratio (length-to-diameter ratio) of up to 1000;[1−6] this offers CNTs an important advantage over conventional fillers. However, for intractable polymers this potential has not been realized, mainly because of the difficulties in the solubility. In solution, strong interactions between the CNTs result in their agglomeration. Different approaches are reported to improve the dispersion of CNTs in solvents or polymers. One of the approaches is the chemical modification of the CNT surface, i.e., functionalization at defect sites. In this method, active sites are introduced onto the surface of CNT by chemical oxidation, for instance, via adding concentrated H_2SO_4 and/or HNO_3.[7] When required, these nanotubes can be functionalized.[8−13] Single-walled carbon nanotubes (SWNTs) and multiwalled carbon nanotubes (MWNTs) functionalized with poly(vinyl alcohol) (PVA) in esterification reactions can be dissolved in highly polar solvents such as DMSO and water.[14] Polystyrene nanocomposites with functionalized SWNTs demonstrated a percolated SWNT network structure with 1.5 wt % of SWNTs, whereas the threshold for a percolated network is 3 wt % for unfunctionalized SWNTs.[15] Even though chemical functionalization of CNTs improve the solubility, the method is relatively complex, especially the procedures of the separation and the collection of functionalized CNTs from byproducts such as amorphous carbon and catalysts.

The dispersion of CNTs in solvents or polymers in the presence of surfactants is another important method that does not require chemical reactions. A single-step solubilization scheme has been developed in which nanotubes are mixed with surfactants in low-power, high-frequency sonicators. This process enhances the exfoliation of CNT bundles without much breakage of the tubes. CNTs are suspended in aqueous media as individuals or bundles surrounded by surfactants[16,17] such as sodium octylbenzenesulfonate and sodium dodecylbenzene sulfate (SDS) or copolymers [18] (or oligomers) such as poly(*m*-phenylenevinylene) (PmPV), poly(aryleneethynylene)s (PEEs), poly(vinylpyrrolidone) (PVP), and Gum Arabic (a highly branched arabinogalactan polysaccharide).[19−21]

CNTs in solutions can be dispersed by dissolving a polymer into the suspended solution. Zhang et al. reported that both the tensile yield strength and the tensile modulus of PVA/PVP/SDS/SWNT are approximately doubled compared to those of PVA.[22] Regev et al.[23] prepared SWNT/SDS/PS composites using latex technology, which exhibit excellent conductive properties with a percolation threshold of 0.28 wt % of SWNTs. Brittain et al. adopted a similar approach for dispersion of silicate in PMMA via in-situ suspension and emulsion polymerization.[24] So far, the preparation of CNT−polymer composites using the surfactant dispersion method is limited to water-soluble polymers or polymers in a latex form. The third method is direct mixing of CNT into the polymer with a twin-screw melt mixer.[25] However, this method is limited for low viscous polymer materials.

† Eindhoven University of Technology.
‡ DSM Research.
§ Donghua University.
* Corresponding author. E-mail: s.rastogi@tue.nl.

10.1021/ma051031n CCC: $33.50
Published on Web 12/16/2005

In this paper, we report a spraying method similar to that is used for surface coatings in industrial applications. To disperse SWNTs on an intractable polymer, for example a linear ultrahigh molecular weight polyethylene (UHMWPE), first an aqueous solution of surfactant/SWNTs is made. The solution is sprayed onto the surface of the as-synthesized fine polymer powder of UHMWPE. The SWNTs in the solution are preferably adsorbed on the surface of the nascent polymer. The polymer having the adsorbed nanotubes is dissolved in xylene. The SWNTs/UHMWPE composites in the form of film are prepared from the solution.[26] Details of the dissolution process of UHMW−PE in solvent, preparation of film from the solution, and its characteristics are described in ref 26. Solution-cast films are drawable in the solid state. Fibers are drawn from these composites. In contrast to the reported rheological studies,[27−31] we observe a minimum in the dynamic viscosity with varying content of nanotubes. The volume effect described by Mackey et al.[32] or selective adsorption of polymer chains on a nanoparticle surface as suggested by Jain et al.[33] provides an explanation for the observed behavior.

2. Experimental Section

Materials. Experiments are carried out on purified HiPco (>95% pure) SWNTs. Two different grades of UHMWPE are used in this study. The two grades are, a commercially available UHMWPE (Montell 1900 LCM) (grade A) with an average molecular weight of $M_w \sim 4 \times 10^6$ g/mol, $M_w/M_n \sim 10$ and a self-synthesized UHMWPE (grade B) with $M_w \sim 4 \times 10^6$ g/mol, $M_w/M_n \sim 2.8$. Details about the self-synthesized PE grade are described in ref 34. Sodium dodecylbenzene sulfate (SDS) is used as a surfactant and xylene as a solvent. Both were purchased from Aldrich.

Characterization Techniques. Environmental scanning electron microscopy (ESEM) is used to observe the resultant morphologies of the nanocomposites. A voltage of 1 kV is used to observe the surface of polymer. Relatively good conducting SWNTs cannot be distinguished in the poor conducting polymer matrix. To enhance the contrast, samples are gold-sputtered.

Oscillatory shear measurements in the linear viscoelastic region are performed using an Advanced Rheometrics Expansion System (ARES). Measurements are carried out using parallel plate geometry (8 mm diameter and thickness 1 mm) at 160 °C under a nitrogen atmosphere. Frequency sweeps with an angular velocity between 0.001 and 100 rad/s are performed in the linear viscoelastic regime at low strain of 1%. Samples are left to equilibrate for 15 min prior to measurement. The obtained values are corrected for the true dimensions between the plates. Electrical conductivity of the nanocomposites is measured at room temperature with a two-probe method.

3. Dispersion of SWNTs in UHMWPE

To disperse SWNTs in UHMWPE, an aqueous solution of SWNTs is prepared using SDS as surfactant, according to a reported method.[23] A 20 mL solution containing 0.044 g of SWNTs and 1 wt % SDS based on H_2O is ultrasonicated for 15 min and then centrifuged at 3000 rpm for 20 min. After sonification, about 90% of SWNTs are suspended in the aqueous solution, whereas the remainder is deposited. The morphology of the suspension of SWNTs is shown in Figure 1. From the figure it may be stated that the SWNTs are dispersed in the form of fine bundles with an average diameter of ∼10 nm. These bundles are rather flexible to coil back, forming loops.

The surface morphology of the nascent (i.e., directly from the reactor) UHMWPE (grade A) used in this work is shown in Figure 2a. Many microconcaves are present on the uneven surface of the polymer powder. This morphology results in enhancement of high surface area, which makes it easy to adsorb microobjects, for example air. Therefore, in the process of casting films, to avoid air bubbles, the adopted first step is to degas air on the surface of the polymer powder by keeping the nascent powder in a vacuum container for an hour.

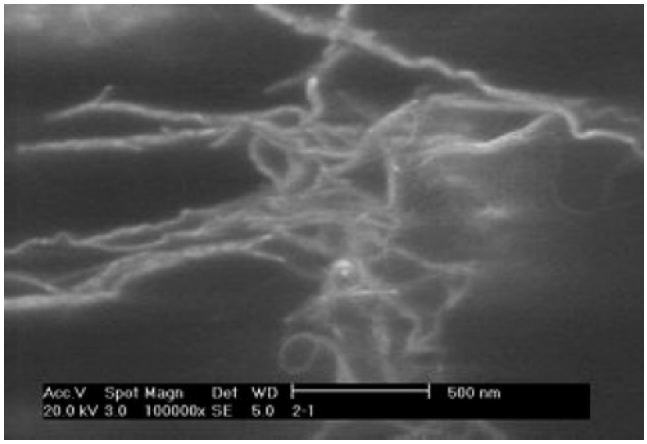

Figure 1. SEM image of SWNTs dispersed in water. SDS is used as a surfactant for the dispersion.

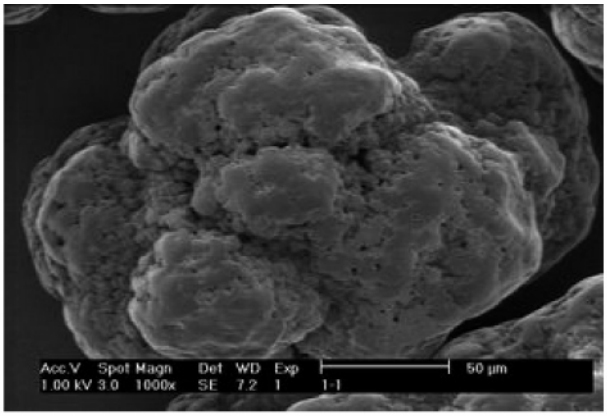

(a)

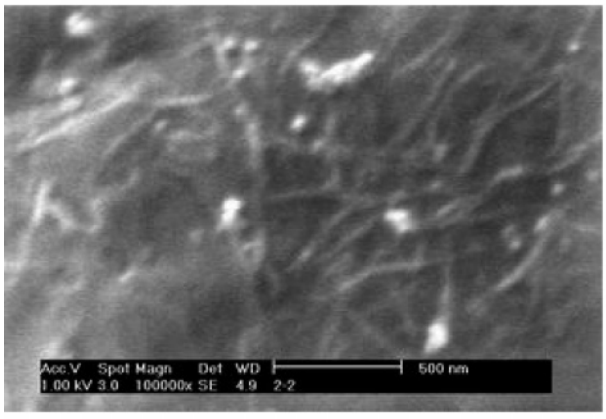

(b)

Figure 2. SEM images of (a) the surface morphology of the nascent UHMWPE (grade A) powder and (b) SWNTs adsorbed on the surface of UHMWPE. The adsorption is achieved after spraying aqueous solution of SWNTs on the UHMWPE surface (∼0.6 wt % of SWNTs on the nascent powder, determined by TGA).

The aqueous solution containing 0.2 wt % of SWNTs is uniformly sprayed on the surface of UHMWPE. On drying, the SWNT-coated polymer powder is obtained. Figure 2b shows that the SWNTs are adsorbed on the surface of the powder. The individual SWNT bundles can be distinguished. The

Figure 3. UHMWPE powders and SWNT−UHMWPE powders, with a weight percentage of 0.1% and 0.6% SWNTs prepared by the spraying technique.

interaction between SWNT and UHMWPE is strong to an extent that when the dried SWNT−UHMWPE powders are immersed into water again, on sedimentation of the powder the water retains its transparency.

Figure 3 presents an image of UHMWPE powders and their blends with different content of SWNTs. Compared to UHMWPE, the coated powders are relatively dark because of the adsorption of the nanotubes on the surface of the polymer powder. The powders become gray when 0.1 wt % of SWNTs is adsorbed and black on the adsorption of 0.6 wt % of SWNTs.

Solution-crystallized films are obtained on dissolving the degassed coated polymer powders at 135 °C in xylene. 0.1 wt % antioxidant based on UHMWPE is added to the solution. The high viscosity of the polymer solution (1 wt % of UHMWPE in xylene) prevents aggregation of the tubes in xylene. The hot solution is quickly transferred to an aluminum tray and left to cool slowly under quiescent conditions. Upon cooling, a gel is formed which is stapled onto a cardboard to prevent lateral shrinkage. The gel is left to dry for a week in a fume hood. The dry film is subjected to the experimental investigation. Obviously, the UHMWPE film without SWNT is transparent, while the film with 0.1 wt % SWNTs shows translucency and the other with 0.6 wt % content is relatively opaque. Details concerning chain mobility below melting temperature in the solution-cast UHMW−PE films are available in ref 26. It is to be noted that tubes without polymer in the solvent xylene tends to aggregate.

4. Solution-Cast Films of SWNT/UHMWPE Nanocomposites

SEM images of the solution crystallized films having SWNT often reveal "shish-kebab" structure, depicted in Figure 4. Shish kebabs are normally observed in extensional flow field where the high molar mass fraction of UHMWPE is extended and crystallizes into a fibrous structure ("shish"). The remaining part that stays in solution as random coil nucleates onto the fibrous structures,[35] forming chain-folded crystals. Formation of shish-kebab-like structures during dissolution of UHMW−PE is described in earlier work of Pennings et al.[35] In SWNT/UHMWPE composites the nanotubes can also form fibrous-like "shish" structure. The folded-chain crystals can directly nucleate onto the nanotube surface. From the SEM pictures alone, Figure 4, it is impossible to make a distinction between the different mechanisms involved in the resultant shish-kebab-like structures. However, we would like to state that the occurrence of such shish-kebab-like structures in the presence of nanotubes increases.

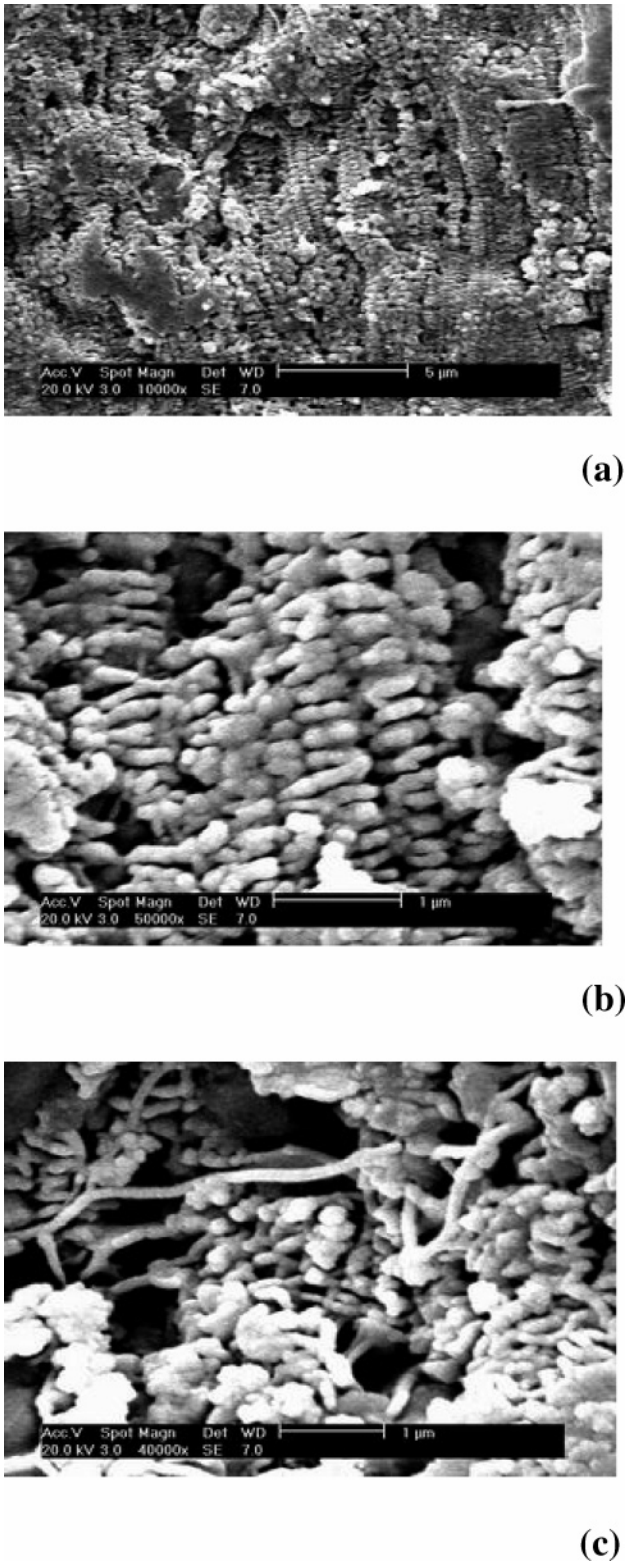

Figure 4. SEM images of 0.6 wt % SWNT/UHMWPE nanocomposites: (a) shish-kebab-like morphology in solution crystallized films of the nanocomposite; (b) and (c) are the magnified regions of (a).

SEM images of the cross section of the solution-crystallized UHMWPE films with 0.6 wt % of SWNTs are shown in Figure 5. The undrawn films exhibit an interesting microstructure. As shown in Figure 5a,b, SWNT bundles are embedded in the UHMWPE matrix. The bundles seemingly have a large diameter of several tens of nanometers. The sample is gold-sputtered because the polymer cannot endure a high voltage, and the applied low voltage of 1 kV results into lower resolution.

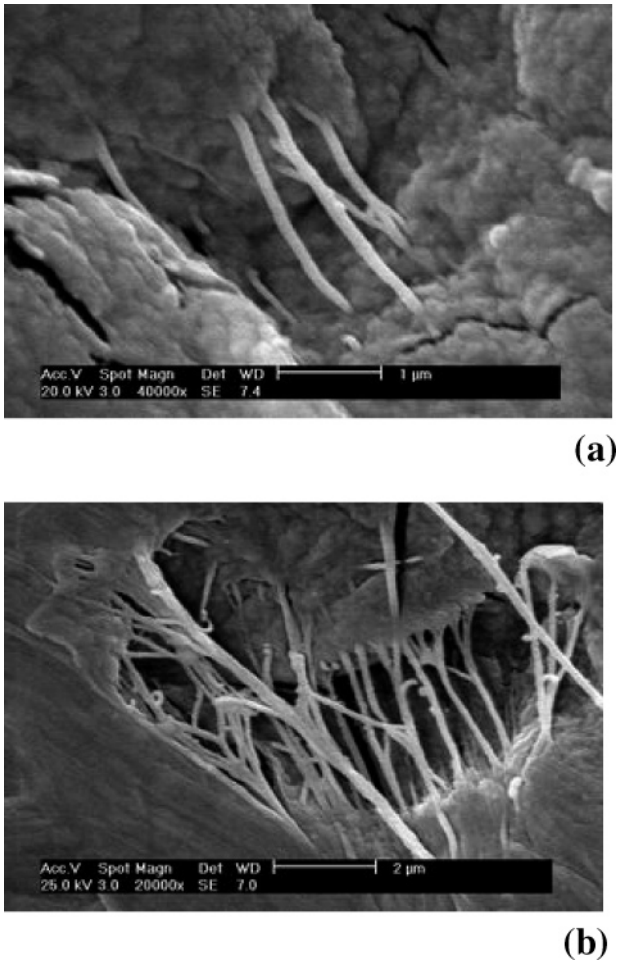

Figure 5. SEM images of the solution crystallized SWNT−UHMWPE nanocomposite films with 0.6 wt % of SWNTs. The image (a) is from the film prior to drawing, and (b) is from the end part of the film drawn at 120 °C.

Therefore, considering the gold layer of about 10 nm, the SWNT bundles are likely to be about 10 nm of the diameter, comparable to the SWNT bundles in aqueous solution shown in Figure 1. Thus, it can be stated that on dissolution of SWNT-coated UHMWPE coagulation of the SWNTs does not occur. The anticipated coagulation process of SWNTs is prevented because of the high viscosity of the UHMWPE solution.

As expected, the SWNTs orient or align upon drawing the composite film made from the xylene solution. Similar to the UHMWPE without nanotubes, the SWNT-coated UHMWPE can be spun from xylene solution. Despite the good drawability and orientation of the SWNTs, the SWNTs/UHMWPE spun fibers do not show any enhancement in mechanical properties.

5. Crystallization of UHMWPE in the Presence of SWNT

The influence of SWNTs during crystallization of UHMWPE is investigated using dynamic rheometry. Compression-molded, SWNT-coated UHMWPE powder samples are left inside the rheometer to relax at 180 °C for an hour. Subsequently, the samples are cooled from 140 to 128 °C at 1 °C/min. At constant strain ($\gamma = 0.1\%$) and frequency ($\omega = 100$ rad/s) isothermal crystallization at 128 °C is followed by measuring the elastic modulus (G'). Khanna[36] and Boutahar[37] related the crystallinity of PE with the scaled modulus G':

$$\frac{\varphi(t)}{\varphi(\infty)} = \frac{G'(t) - G'(0)}{G'(\infty) - G'(0)}$$

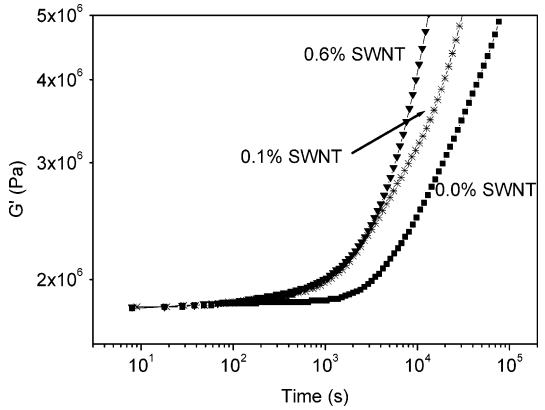

Figure 6. Isothermal crystallization (128 °C) of SWNTs/UHMWPE composites at constant strain and frequency.

Table 1. Onset and Crystallization Rate of Polyethylene in SWNT/UHMWPE Composite (Quantitative Data from Figure 6)

content of SWNTs (wt %)	onset of crystallization (s)[a]	crystallization rate (%/s)[b]
0.0	1000	5.45×10^{-3}
0.1	210	17.4×10^{-3}
0.6	140	53.7×10^{-3}

[a] Determined at 1% of the total crystallinity within the given time of the experiment. [b] Determined at 50% of the total crystallinity within the given time of the experiment.

where $G'(0)$ is the initial modulus and $G'(\infty)$ is the plateau value reached at the end of crystallization. $\varphi(t)$ is the degree of crystallinity at time t, and $\varphi(\infty)$ is the maximum degree of crystallinity of the samples.

Figure 6 shows that upon increasing the SWNT content in the composite the onset of crystallization occurs earlier. Also, the speed of crystallization is faster with increasing amount of the SWNTs. Table 1 shows that the onset of crystallization is 5 times earlier and 3 times faster when 0.1 wt % of SWNTs is added to UHMWPE. Considering the applied low strain (0.1%), the enhancement of nucleation/crystallization on addition of SWNTs suggests that the "shish-kebab" structure, shown in Figure 4, is not due to the orientation of the high molar mass fraction but is likely a result of the crystallization of the polymer chains onto the nanotube surface, where the SWNT surface acts as a nucleation site for PE chains to crystallize.

6. Influence of SWNTs on the UHMWPE Melt

Oscillatory shear measurements are performed on samples in the viscoelastic region at low strain ($\gamma = 1\%$) at different frequencies ($\omega = 10^{-3}-10^{2}$ rad/s) and temperatures ranging between 160 and 220 °C. The master curves are obtained by using the time−temperature superposition principle. Since the SDS concentration in the nanocomposites is similar to the tube concentration, first the experiments are performed to study the influence of SDS on UHMWPE. From Figure 7, it is evident that there is no measurable influence of SDS on the rheological behavior of UHMWPE on SDS loadings ranging from 0.1 to 1 wt %. In the 5 wt % SDS sample a decrease in storage modulus is observed (7%), were the phase angle remains unchanged.

However, on dispersing SWNTs with SDS in UHMWPE, a complicated rheological situation arises that may be attributed to interactions between polymer and nanotubes; such interactions are described in ref 30 and reproduced here in Figure 8.

To recall, in Figure 8 (a) depicts SWNT−SWNT network due to overlap of two nanotubes, (b) a PE−SWNT network where the polymer may be entangled or adsorbed on the nanotube, (c) depicts SWNT bridging by polymer, and (d) refers

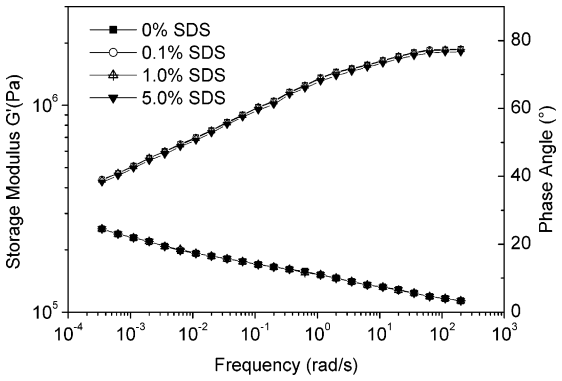

Figure 7. Storage modulus G' of UHMWPE with varying concentration of SDS surfactant.

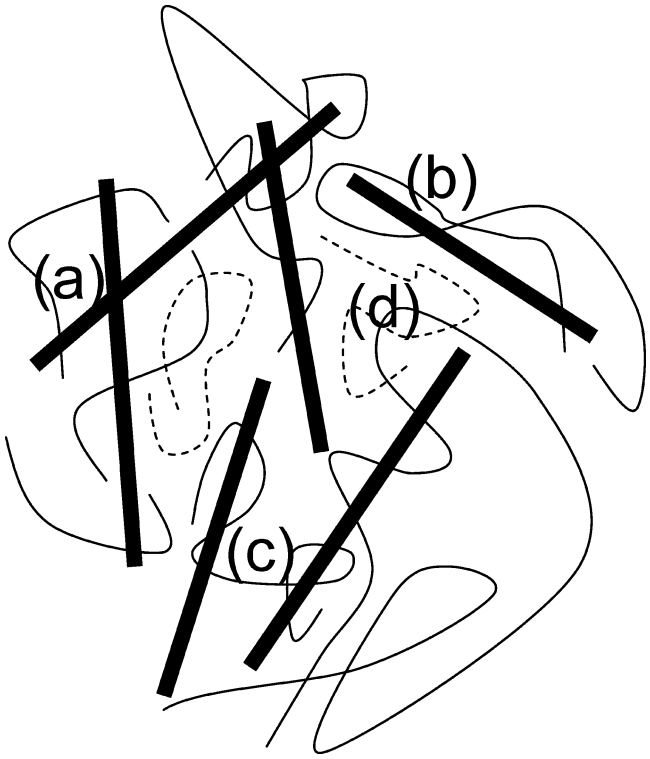

Figure 8. Illustration of nanotube−polymer interactions. The figure depicts presence of different networks: nanotube−nanotube network formation (a), nanotube−polymer interaction (adsorption) (b); nanotube−polymer−nanotube bridging (c); polymer−polymer network (d) (from ref 30).

to polymer network formation in the polymer matrix through temporary entanglements.

Figure 9a shows master curves for storage modulus at 160 °C varying from 0 to 0.2 wt % of SWNT/UHMWPE composite. The figure is divided into two regions, region I and region II. In region I, considering the high molecular weight ($\sim 4 \times 10^6$ g/mol) of the polymer, the probing time in the experiment is too short for chains to relax. Therefore, UHMWPE behaves rubberlike, and G' is nearly independent of frequency. The resulting plateau modulus is a combination of the elastic polymer network and elastic nanotube network.

In region II which lies at low frequencies, a striking observation is that at these low frequencies the storage modulus decreases considerably with an addition of low amount of SWNTs in the UHMWPE ranging from 0.05 to 0.2 wt %. Whereas at high frequencies (100 rad/s), in region I, the storage modulus also decreases but to a much lesser extent.

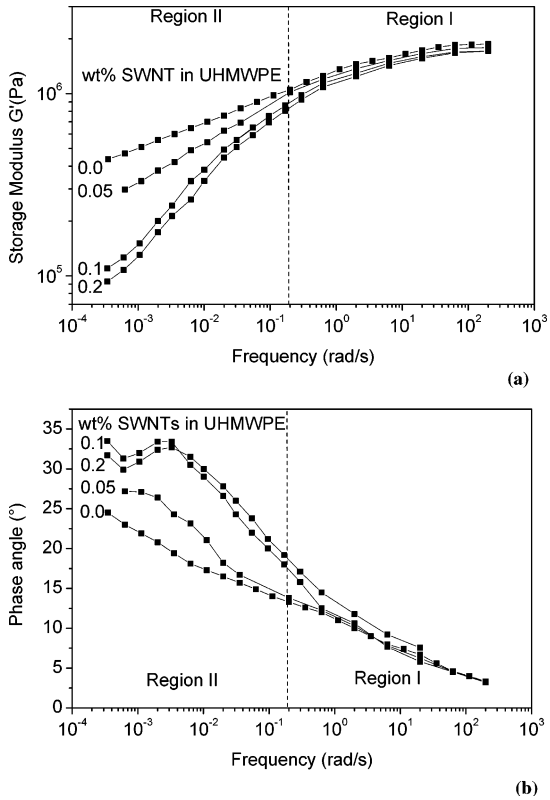

Figure 9. (a) Storage modulus G' of UHMWPE with varying SWNT content of 0−0.2 wt % at 160 °C. **(**b) Phase angle of UHMWPE with varying SWNT content of 0−0.2 wt % at 160 °C.

The phase angle, δ, for the different compositions of SWNTs is depicted in Figure 9b. It is seen that upon increasing the amount of SWNTs from 0 to 0.1 wt % the phase angle increases in region II, indicating that the composite behaves less elastic than the pure polymer. To our knowledge, there are no studies that report the observed decrease in storage modulus for such a low loadings of nanotubes. But similar effects are reported in some recent studies when nanofillers (particle size 0.5−3 nm) are blended with linear polymers.[32,33,38]

On increasing the SWNT content beyond 0.2 wt %, the storage modulus at low frequencies becomes independent of frequency, showing a second plateau in region II (see Figure 10a). It is known from the literature that interconnected structures of anisiometric fillers result in an apparent yield stress which is visible in the dynamic measurements by a second plateau, as seen in region II.[41] The interconnected structure (nanotube network) is described as (a) in Figure 8. In the Figure 10a, the second plateau is observed at low loading of 0.6 wt % of SWNTs. With increasing amount of SWNTs in the polymer matrix the second plateau modulus increases. This increase is attributed to more pronounced connectivity of the nanotubes.

The phase angle depicted in Figure 10b shows a subsequent decrease with the increasing amount of SWNTs in region II. The phase angle goes through a maximum. The frequency at which the phase angle shows a maximum increases with increasing amount of SWNTs in the polymer matrix. Shift of the maximum to higher frequencies indicates a more dominant nanotube network with increasing SWNTs concentration. The presence of a maximum also suggests a change in the viscoelastic response with frequency, i.e., from viscous to elastic like response on going from region II to region I.

These observations are similar to liquid-to-solid or liquid-to-gel transitions observed by Winter et al.[39] in their gel studies. Similar effects have been reported for melt mixed polypropy-

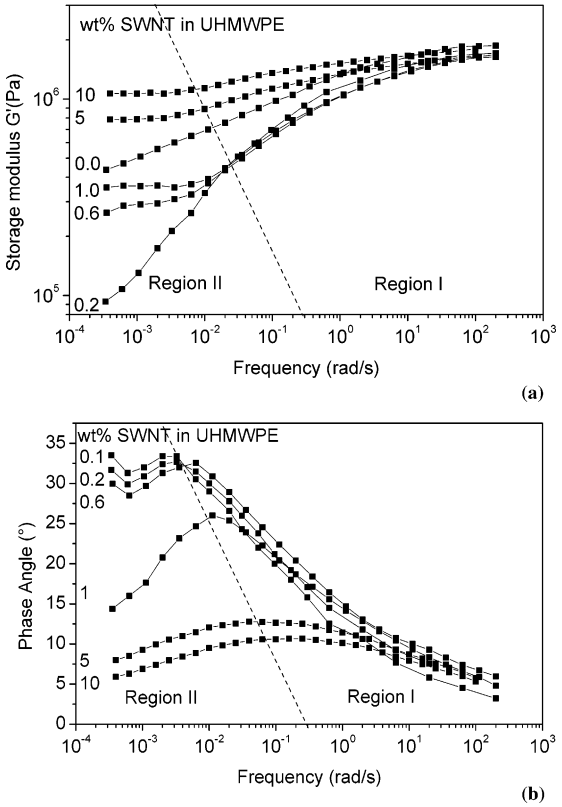

Figure 10. Storage modulus G' and phase angle of UHMWPE with different concentrations of SWNTs at 160 °C. (a) The storage modulus varies with the amount of nanotubes. Distinct variations at low and high frequencies are observed in region II and region I, respectively. The corresponding changes in the phase angle are depicted in (b).

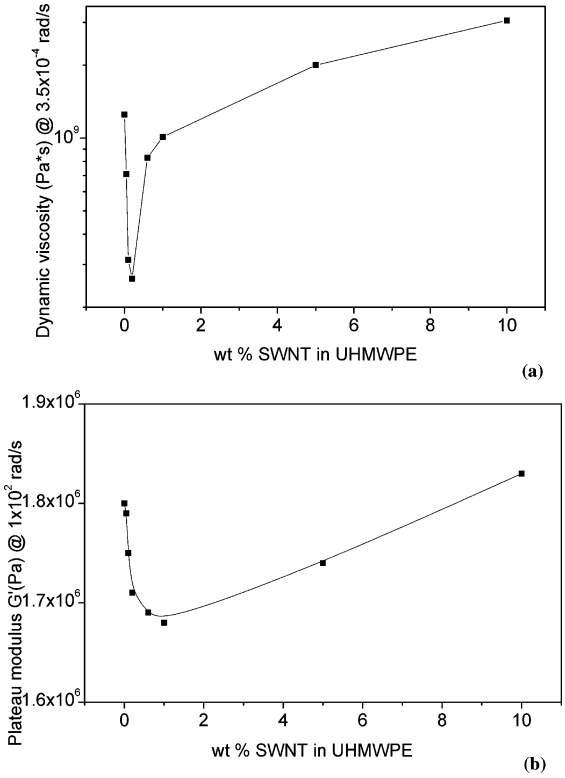

Figure 11. Figure depicts changes in dynamic viscosity and plateau modulus with the varying concentration of nanotubes. (a) Dynamic viscosity in region II at 0.000 35 rad/s of the SWNT/UHMWPE (grade A) nanocomposites shows significant drop with the addition of 0.1−0.2 wt % of SWNTs. (b) Plateau modulus in region I at 100 rad/s of the SWNT/UHMWPE nanocomposites also registers a minimum in the modulus with increasing concentration of SWNTs.

lene/MWNT[27] composites, polycarbonate/MWNT composites,[28] and polyamide 6/MWNT composites.[29]

The distinct minimum in dynamic viscosity with the varying amount of SWNTs becomes more evident in Figure 11a where the dynamic viscosity at low frequency (3.5×10^{-4} rad/s) is shown as a function of SWNTs content. The figure depicts a minimum in the dynamic viscosity at 0.1−0.2 wt % of SWNTs. The variation in the storage or plateau modulus as a function of SWNTs content at high frequency (100 rad/s) is given in Figure 11b. The plateau modulus decreases up to ∼1 wt %, after which the modulus increases.

The minimum in storage modulus (or dynamic viscosity) with increasing amount of SWNTs, at both high and low frequencies, requires an explanation. What follows is a possible explanation for the drop in the viscosity at relatively low content of nanotubes.

First, we recall that UHMWPE used for the present studies has a broad molar mass distribution. Because of the van der Waals interaction PE chains tend to be adsorbed on the nanotubes (also suggested by the crystallization studies, see Figure 6). Within the experimental time frame the probability of the high molar mass to remain adsorbed on the nanotubes will be higher than the low molar mass chains. The adsorbed polymer, especially of high molar mass, can be considered as an immobilized part of the nanotube at least for times larger than the experimental time. Thus, the polymer forming the remaining matrix will effectively have a lower average molecular weight than the pure polymer (dashed chains in the illustration of Figure 8). This would cause faster relaxation of chains thus a decrease in the storage modulus (or viscosity) and subsequently a higher phase angle, as depicted in Figure 9. The observed drop in viscosity at such a low concentration of filler is in agreement with recent findings reported elsewhere. To quote, Mackey et al.[32] reported decrease in viscosity in polystyrene filled with cross-linked polystyrenes, whereas Jain et al.[33] observed a similar drop in viscosity using silica nanoparticles as filler. In nanocomposites filled with silica, an explanation provided for the viscosity drop was the selective physicoadsorption of polymer chains onto nanoparticles surfaces. Independently, preferential adsorption of high molar mass component in polydisperse UHMW−PE on silica particles was observed by Maurer et al.[40]

When the nanotube content is increased beyond 0.2 wt %, the nanotube network is formed. The formation of this network gets evident from the appearance of the plateau region at lower frequencies. The elastic strength of this network increases with increasing amount of the nanotubes.

To strengthen the concepts on selective adsorption of high molecular weight fraction, experiments are performed on a grade (grade B) having molecular weight similar to grade A but a lower polydisperisty, i.e., 2.8 instead of ∼10. Figure 12 shows that similar to grade A (Figure 10) the storage modulus in region II of grade B becomes independent of frequency at a SWNTs concentration of 0.6 wt %. This implies the formation of a mechanical nanotube network. However, unlike grade A, grade B does not show a minimum in the storage modulus in region II. This can be explained by the difference in polydisperisty; since in grade B all polymer chains are relatively long ($M_n \sim 1.3 \times 10^6$ g/mol) and are of similar length, no clear distinction in the molecular weight between the polymer matrix before and after the adsorption of chains to nanotubes exist. Therefore, increasing the nanotube content simply results into a stronger nanotube network.

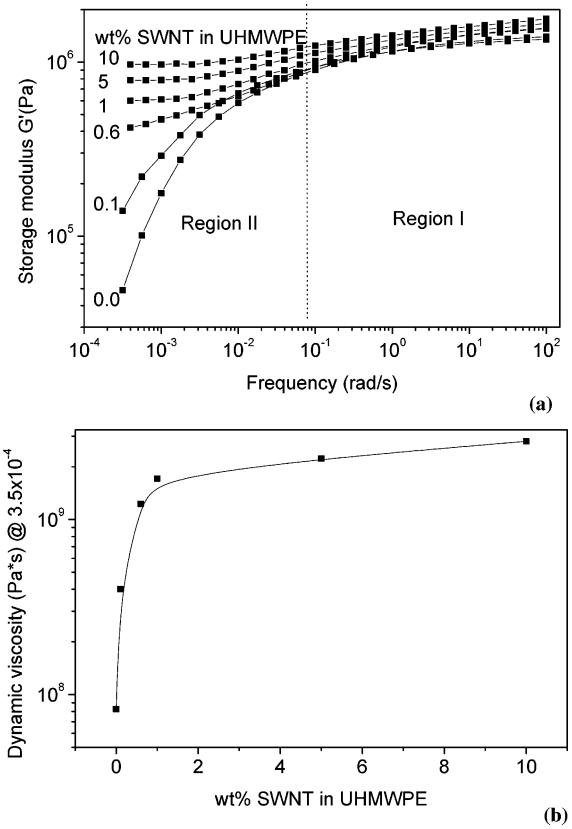

Figure 12. Storage modulus G' of SWNTs/UHMWPE (grade B) at 160 °C. (a) The modulus as a function of frequency and wt % of SWNTs. (b) Storage modulus at 0.000 35 rad/s (region II) with different wt % of SWNTs.

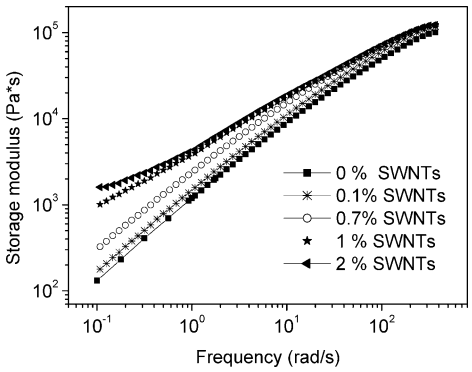

Figure 13. Storage modulus G' of SWNTs/HDPE at 160 °C as a function of frequency and wt % of SWNTs. Molar mass of HDPE is 100 000 and molar mass distribution of 4.

In addition to it, many reported studies in the literature also do not observe the drop in dynamic viscosity.[27−32] Since in the literature composites with lower molecular weight are investigated (less than 400 000 g/mol), it seems plausible that a critical molecular weight of the polymer exists to notice the preferred adsorption mechanism. For example, in low molecular weight polymer the polymer/nanotube interaction (for the given experimental time) will be sufficiently small, which favors easier desorption of polymer from the nanotube surface. Results in Figure 13 describe our observations on a commercial HDPE grade, having a molecular weight of 100 000 g/mol and a polydispersity of 4. Similar to the results reported in the literature, no decrease in viscosity is observed. When compared to the UHMWPE studies, these results strengthen the hypothesis that preferred adsorption can be noticed only when a chain is sufficiently long to remain adsorbed on the nanotubes. Similar

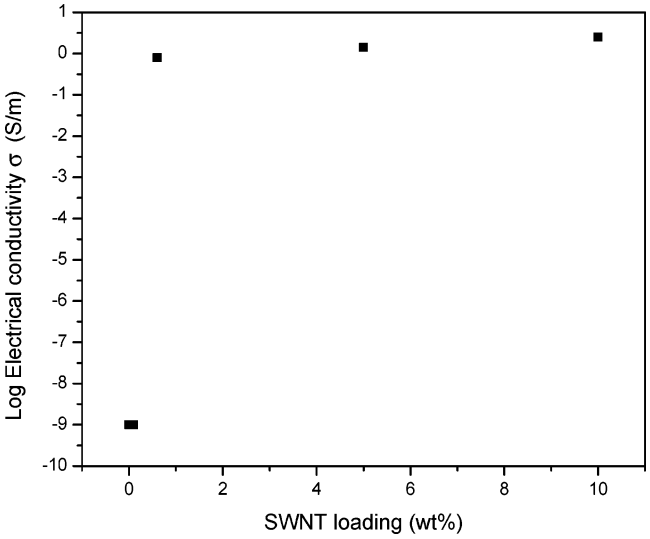

Figure 14. Electrical conductivity of SWNTs/UHMWPE nanocomposites (grade B).

to Figures 10a and 12a, in Figure 13 increase in modulus at low frequencies on higher loadings is attributed to the nanotube network formation.

In Figures 10 and 12, the second plateau modulus in region II at low frequencies of the SWNTs/UHMWPE polymer network ranges between 4×10^5 and 6×10^5 Pa for 0.6−1.0 wt % of SWNTs. This network modulus is higher than that reported in the literature for similar CNT loadings in a relatively low molar mass polymer. Pötschke et al.[30] associated the origin of the modulus to the network formation between the carbon nanotubes linked by the polymer chains (polymer nanotube bridging (c) in Figure 8). In the case of SWNTs/UHMWPE nanocomposites the origin of the high modulus can be explained by the stronger polymer−nanotube interaction compared to the low molar mass nanotube composites. This can be simply explained by considering the fact that the diameter of a random coil of UHMWPE is estimated over 120 nm, whereas the diameter of SWNTs ranges between 6 and 10 nm. Considering the large radius of gyration of UHMWPE compared to the diameter of SWNTs, the polymer chains are likely to entangle with the nanotubes. Thus, the nanotubes that are in proximity can be easily connected by the long polymer chains. This is likely to result in a decrease in chain mobility and an enforcement of the nanotube network by the polymer chain. Since the molecular weight of the polymers (∼4 000 000 g/mol) used in our studies is considerably higher compared to that reported for low molar mass (50 000−150 000 g/mol), bridging of the nanotubes with the polymer is more likely to happen at lower nanotube concentration. In addition to it, the number of interactions for a long chain with the nanotubes will be higher for the same loading of nanotubes in the low molar mass polymer.

Experiments reported above clearly demonstrate that the viscoelastic response of polymer/CNT composites is strongly influenced by the polydispersity. The simple spraying technique used to obtain the UHMWPE nanocomposites opens an opportunity to overcome the intractable problem of UHMWPE. In future publications we will address a more in-depth study to investigate the mechanism behind the observed rheological behavior.

7. Electrical Conductivity of SWNTs/UHMWPE Nanocomposites

Figure 14 shows that the SWNT/UHMWPE nanocomposites are conductive at a SWNT loading of 0.6 wt %. It is generally

accepted that when the nanotube loading reaches the conductivity threshold, a conductive network exists in which the nanotubes form a conductive path. For or a conductive network to be formed, nanotubes do not require real overlap of the nanotubes, since a conductive network can be formed through hopping and tunneling processes. However, further increase in SWNT content to 1 wt % or higher does not show a pronounced increase in conductivity; there it is assumed that the network is formed by geometrical overlapped nanotubes at 0.6 wt % SWNTs. Experiments reported in this paper show that the threshold for the mechanical network formation, which is probed from rheology, is in agreement with the sudden increase in electrical conductivity. On the other hand, for low molar mass polymers electrical percolation is noticed earlier than the mechanical percolation. This difference in the high and low molar mass polymers may be simply attributed to the chain lengths. In the low molar mass polymers greater amount of nanotubes are required to bridge polymer−nanotube network compared to the high molar mass polymers.[27,42] However, the low threshold for rheological changes and electrical properties reported in this paper are comparable to that reported for other nanotube composites. This indicates that the simple spraying technique is adequate to generate a well-dispersed SWNTs/UHMWPE composite. The threshold value for percolation can be further lowered with improved dispersion of SWNTs in a solvent.

8. Conclusion

A new simple method of spraying SWNTs on the surface of UHMWPE particles is used to prepare SWNTs/UHMWPE nanocomposites. Considering the simplicity of the technique, this method can be applied in general. The UHMWPE coated with the nanotubes is dissolved in xylene. It is shown that in solution due to the high viscosity of the UHMWPE the SWNTs do not coagulate. SEM images reveal a good distribution of the SWNTs in the polymer matrix after crystallization from the solution. The "shish-kebab" type of morphology observed in these films suggests that the nanotubes act as a nucleating agent for the polymer chains. This is further strengthened by following crystallization behavior from the melt, using oscillatory rheometry as a tool. The observations are that the onset of crystallization and the crystal growth rate enhances considerably with increasing concentration of nanotubes in the polymer matrix. For an example, isothermal crystallization probed by rheometry shows enhancement in crystallization by a factor of 3 at low loadings of 0.1 wt % of SWNTs. Solution-casted films having a concentration of SWNTs less than 3% are drawable. However, the drawability decreases with increasing concentration of SWNTs.

Conductivity and linear viscoelastic measurements reveal that a threshold of 0.6% of SWNTs is required to form a nanotube network within the polymer matrix. This threshold value is comparable to other SWNTs−polymer composites reported in the literature.[27−31] This proves that the adopted spraying technique in the intractable UHMWPE is effective. The resulting network increases electrical conductivity by 9 orders of magnitude.

The network formation that occurs in the melt from and above 0.6 wt % of SWNTs dispersed in polymer is observed as a plateau modulus at low frequency in the oscillatory shear measurements. The strength of the network increases with increasing concentration of the nanotubes.

A comparison with the reported data on the SWNTs/polymer network modulus for the same concentration of SWNTs shows that the strength of the network formed in UHMWPE is higher than that for the low molecular weight polymers. A plausible explanation of the higher network modulus is that the high molecular weight polymers will have higher probability to entangle with the dispersed nanotubes. This results in a stronger network formation at low loadings of SWNTs compared to the reported data on polymer/CNT composites.

The polydisperisty of UHMWPE in nanocomposites has a distinct impact on the viscoelastic behavior of the nanocomposites. The observations are that in a polydisperse UHMWPE sample with increasing concentration of SWNTs a clear minimum exists in dynamic viscosity (modulus). However, such a minimum is not realized in a sample having a relatively sharp molar mass distribution. Selective adsorption of the high molar mass fraction on the dispersed SWNTs seems to be a possible explanation for the observed minimum. Because of the selective adsorption of the high molar mass, the apparent molar mass of the polymer matrix decreases; consequently, the phase angle shows a more viscous-like response as anticipated for the lower molar mass.

References and Notes

(1) Ijima, S. *Nature* (*London*) **1991**, *354*, 603.
(2) Bethune, D. S.; Kiang, C. H.; De Vries, M. S.; Gorman, G.; Savoy, R.; Vazque, Z.; Beyers, R. *Nature* (*London*) **1993**, *363*, 605.
(3) Yakobson, B. I.; Smalley, R. E. *Science* **1997**, *85*, 324.
(4) Kong, J.; Franklin, N.; Zhou, C.; Chapline, M. A.; Peng, S.; Cho, K.; Dai, H. *Science* **2000**, *287*, 622.
(5) Walters, D. A.; Ericson, L. M.; Casavant, M. J.; Liu, J.; Colbert, D. T.; Smith, K. A.; Smalley, R. E. *Appl. Phys. Lett.* **1999**, *74*, 3803.
(6) Baughman, R. H.; Zakhidov, A. A.; de Heer, W. A. *Science* **2002**, *297*, 787.
(7) Shaffer, M. S. P.; Fan, X. F.; Windle, A. H. *Carbon* **1998**, *36*, 6, 1603.
(8) Eitan, A.; Jiang, K.; Dukes, D.; Andrews, R.; Schadler, L. S. *Chem. Mater.* **2003**, *15*, 3198.
(9) Rinzler A. G.; Lui, J.; Dai, H.; Lui, H.; Nikolaev, P.; Huffman, F. J.; Rodriguez-Macias, F. J.; Boul, P. J.; Lu, A. H.; Heymann, D.; Colbert, D. T.; Lee, R. S.; Fischer, J. E.; Rao, A. M.; Eklund, P. C.; Smalley, R. E. *Appl. Phys.* **1998**, *67*, 29.
(10) Chen, J.; Hamon, M. A.; Hu, H.; Chen, Y.; Rao, A. M.; Eklund, P. C.; Haddon, R. C. *Science* **1998**, *282*, 95.
(11) Viswanathan, G.; Chakrapani, N.; Yang, H.; Wei, B.; Chung, H.; Cho, K.; Ryu, C. Y.; Ajayan, P. M. *J. Am. Chem. Soc.* **2003**, *125*, 9258.
(12) Hill, D. E.; Lin, Y.; Rao, A. M.; Allard, L. F.; Sun, Y.-P. *Macromolecules* **2002**, *35*, 9466.
(13) Lin, Y.; Zhou, B.; Fernando, K. A. S.; Liu, P.; Allard, L. F.; Sun Y.-P. *Macromolecules* **2003**, *36*, 7199.
(14) Shaffer, M. S. P.; Windle, A. H. *Adv. Mater.* **1999**, *11*, 93.
(15) Mitchell, C. A.; Bahr, J. L.; Arepalli, S.; Tour, J. M.; Krishnamoorti, R. *Macromolecules* **2002**, *35*, 8825.
(16) Islam, M. F.; Eojas, E.; Bergey, D. M.; Johnson, A. T.; Yodh, A. G. *Nano Lett.* **2003**, *3*, 269.
(17) Moore, V. C.; Strano, M. S.; Haroz, E. H.; Hauge, R. H.; Smalley, R. E. *Nano Lett.* **2003**, *3*, 1379.
(18) Levi, N.; Czerw, R.; Xing, S.; Iyer, P.; Carroll, D. L. *Nano Lett.* **2004**, *4*, 1267.
(19) Bandyopadhyaya, R.; Nativ-Roth, E.; Regev, O.; Yerushalmi-Rozen, R. *Nano Lett.* **2002**, *2*, 25.
(20) Chen, J.; Liu, H.; Weimer, W. A.; Halls, M. D.; Waldeck, D. H.; Walker, G. C. *J. Am. Chem. Soc.* **2002**, *124*, 9034.
(21) Ausman, K. D.; Piner, R.; Lourie, O.; Ruoff, R. S.; Korobov, M. *J. Phys. Chem. B* **2000**, *104*, 8911.
(22) Zhang, X.; Liu, T.; Sreekumar, T. V.; Kumar, S.; Moore, V. C.; Hauge, R. H.; Smalley, R. E. *Nano Lett.* **2003**, *3*, 1285.
(23) Regev, O.; Elkati, P. N. B.; Loos, J.; Koning, C. E. *Adv. Mater.* **2004**, *16*, 248.
(24) Huang, X.; Brittain, W. J. *Macromolecules* **2001**, *34*, 3255.
(25) Bhattacharyya, A. R.; Potschke, P.; Abdel-Goad, M.; Fischer, D. *Chem. Phys. Lett.* **2004**, *392*, 28.
(26) Smith, P.; Lemstra, P. J. *J. Mater. Sci.* **1980**, *15*, 505. Rastogi, S.; Spoelstra, A. B.; Goossens, J. G. P.; Lemstra, P. J. *Macromolecules* **1997**, *30*, 7880.
(27) Kharchenko, S. B.; Douglas, J. F.; Obrzut, J.; Grulke, E. A.; Migler, K. *Nat. Mater.* **2004**, *3*, 564.
(28) Pötschke, P.; Fornes, T. D.; Paul, D. R. *Polymer* **2002**, *43*, 3247.
(29) Meincke, O.; Kaempfer, D.; Weickmann, H.; Friedrich, C.; Vathauer, M.; Wart, H. *Polymer* **2004**, *45*, 739.

(30) Pötschke, P.; Abdel-Goad, M.; Alig, I.; Dudkin, S.; Lellinger, D. *Polymer* **2004**, *45*, 8863.
(31) Du, F.; Scogna, R. C.; Zhou, W.; Brand, S.; Fischer, J. E.; Winey, K. I. *Macromolecules* **2004**, *37*, 9048.
(32) Mackay, M. E.; Dao, T. T.; Tuteja, A.; Ho, D. L.; Brooke van, H.; Kim, H. C.; Hawker, C. J. *Nat. Mater.* **2003**, *2*, 762.
(33) Jain, S. H. Nano-scale events with macroscopic effects in polypropylene/silica nanocomposites; effect of polymer adsorption on processability and properties. Ph.D. Thesis,Technische Universiteit Eindhoven, 2005 (http://alexandria.tue.nl/extra2/200511823.pdf).
(34) Garkhail-Sharma, K. Easily processable ultrahigh molecular weight polyethylene with narrow molecular weight distribution. Ph.D. Thesis, Technische Universiteit Eindhoven, 2005 (http://alexandria.tue.nl/extra2/200510552.pdf).
(35) Pennings, A.; Kiel, A. M. *Kolloid Z. Z. Polym.* **1965**, *205* 160.
(36) Khanna, Y. P. *Macromolecules* **1993**, *26*, 3639.
(37) Boutahar, K.; Carrot, C.; Guillet, J. *Macromolecules* **1998**, *31*, 1921.
(38) Roberts, C.; Cosgrove, T.; Schimidt, R. G.; Gordon, G. V. *Macromolecules* **2001**, *34*, 538.
(39) Winter, H. H.; Mours, M. *Adv. Polym. Sci.* **1997**, *134*, 165.
(40) Maurer, F. H. J.; Schoffeleers, H. M.; Kosfeld, R.; Uhlenbroich, T. H. *Prog. Sci. Eng. Compos.* **1992**, 803.
(41) Shenoy, A. V. *Rheology of Filled Polymer Systems*; Kluwer Academic Publishers: Dordrecht, 1999.
(42) Ramanathan, T.; Liu, H.; Brinson, L. C. *J. Polym. Sci., B: Polym. Phys.* **2005**, *43*, 2269.

MA051031N